Conformation of Manganese(II)−Nucleotide Complexes Bound to Rabbit Muscle Creatine Kinase: ^{13}C NMR Measurements Using [2-^{13}C]ATP and [2-^{13}C]ADP†

Bruce D. Ray,‡ Mei H. Chau,‡ Wilmer K. Fife,§ Gotam K. Jarori,‡,|| and B. D. Nageswara Rao*,‡

Department of Physics and Department of Chemistry, Indiana University Purdue University Indianapolis (IUPUI), 402 North Blackford Street, Indianapolis, Indiana 46202-3273

Received February 1, 1996; Revised Manuscript Received April 8, 1996⊗

ABSTRACT: Conformations of cation−nucleotide complexes bound to rabbit muscle creatine kinase were investigated by measuring paramagnetic effects on ^{13}C spin relaxation in E·Mn[2-^{13}C]ATP and E·Mn[2-^{13}C]ADP at three different frequencies, viz., 50, 75, and 125 MHz, and as a function of temperature in the range of 7−35 °C (at 75 MHz). Arrhenius plots of the temperature dependencies of relaxation rates show a positive slope with low activation energies of 1.3 ± 0.2 kcal/mol and 2.0 ± 0.2 kcal/mol for E·Mn ATP and E·MnADP, respectively. The relaxation rates of both complexes show strong frequency dependence, indicating that these rates are not exchange limited. Analysis of the data yields Mn(II)−2C distances of 10.0 ± 0.5 Å for E·MnATP and 8.6 ± 0.5 Å for E·MnADP. These data were interpreted, along with previously published information, on the location of the cation with respect to the phosphate chain [Jarori, G. K., Ray, B. D., & Nageswara Rao, B. D. (1985) *Biochemistry 24*, 3487−3494], and on the adenosine conformation [Murali, N., Jarori, G. K., & Nageswara Rao, B. D. (1993) *Biochemistry 32*, 12941−12948] in these complexes. The Mn(II)−2C distances depend on the orientation of the phosphate chain relative to the adenosine moiety. Conformational searches were performed by varying the two torsion angles, $\phi_1(C_{4'}-C_{5'}-O_{5'}-P_\alpha)$, and $\phi_2(C_{5'}-O_{5'}-P_\alpha-O_{\alpha\beta})$, along with CHARMm energy computations, in order to determine acceptable conformations compatible with the distances determined. The significant difference in the Mn(II)−2C distances in E·MnATP and E·MnADP is indicative of the structural alterations occurring at the active site as the enzyme turns over.

Enzymes utilizing ATP[1] as a substrate occur in a variety of critical cellular processes and may be classified into three groups, viz., phosphoryl transfer, adenyl transfer, and pyrophosphoryl transfer enzymes. All three categories of these enzymes require Mg(II) as an obligatory component of their reaction complexes *in vivo*. Most of them are activated *in vitro* by substituent paramagnetic cations Mn(II) and Co(II). Therefore, paramagnetic enhancement of spin-relaxation rates of nuclei, proportional to the reciprocal sixth power of their distances from the cation, offered a convenient method to deduce the conformations of the reaction complexes bound to ATP-utilizing enzymes (Mildvan & Gupta, 1978; Villafranca, 1984). Such information is of considerable value in elucidating the mechanisms of these reactions.

An isolated ATP molecule has three internal mobilities: glycosidic reorientation of the adenine base, ribose pucker, and the internal flexibility and overall reorientational motion of the phosphate chain (Nageswara Rao & Ray, 1992). A determination of the conformation of the cation−nucleotide complex thus requires structural data that will reveal how the internal motions are arrested in the bound species. This data may be gathered by a two-pronged approach of (a) utilizing proton TRNOESY measurements to determine the glycosidic torsion and ribose pucker and (b) acquiring distance data on substrate nuclei, with reference to the cation, by means of the paramagnetic enhancement in their relaxation rates.

Conformational studies of cation−nucleotide complexes bound to ATP-utilizing enzymes by magnetic resonance techniques have been in vogue for sometime. In the case of creatine kinase complexes, Mclaughlin *et al*. (1976) suggested the intriguing possibility of an α,β-bidentate complex for bound MnATP. However, this result was superceded by the work of Reed and co-workers (Reed & Leyh, 1980; Leyh *et al*., 1985), who made elegant use of superhyperfine interactions between Mn(II) and ^{17}O in labeled nucleotides to demonstrate an α,β,γ-tridentate complex for MnATP and an α,β-bidentate complex for MnADP bound to creatine kinase. Similar results were obtained for 3-*P*-glycerate kinase (Moore & Reed, 1985). ^{31}P spin-relaxation measurements in enzyme-bound nucleotide complexes of several kinases in the presence of Co(II) have been used to establish that the cation is directly coordinated to the phosphate groups. The enzymes studied include creatine kinase (Jarori *et al*., 1985), 3-phosphoglycerate kinase (Ray

† Supported in part by grants from National Institutes of Health (GM43966) and IUPUI. Purdue Biochemical Magnetic Resonance Laboratory was partially supported by RR01077. Parts of this work have been presented at XIII International Conference on Magnetic Resonance in Biological Systems, Madison, WI (August 14−19, 1988), and at the Joint Meeting of Biophysical Society and American Society for Biochemistry and Molecular Biology, Houston, TX (February 9−13, 1992).

* Author to whom correspondence should be addressed.

‡ Department of Physics.

§ Department of Chemistry.

|| Permanent address: Tata Institute of Fundamental Research, Homi Bhabha Road, Colaba, Bombay 400 005, India.

⊗ Abstract published in *Advance ACS Abstracts*, May 15, 1996.

[1] Abbreviations: ADP, adenosine 5′-diphosphate; ATP, adenosine 5′-triphosphate; E·M·S, enzyme−metal−substrate; E·S, enzyme−substrate; Hepes, *N*-(2-hydroxyethyl)piperazine-*N*′-2-ethanesulfonic acid; NMR, nuclear magnetic resonance; NOE, nuclear Overhauser effect; TRNOESY, two-dimensional (2D) transferred NOE spectroscopy.

S0006-2960(96)00257-7 CCC: $12.00

& Nageswara Rao, 1988a,b), adenylate kinase[2] (Ray *et al*., 1988), and arginine kinase (Jarori *et al*., 1989).

Proton TRNOESY measurements have been used to deduce the adenosine conformation of MgATP and MgADP bound to creatine kinase (Murali *et al*., 1993), arginine kinase (Murali *et al*., 1994), and pyruvate kinase (Jarori *et al*., 1994) and of MgATP bound to the adenyl transfer enzyme, methionyl tRNA synthetase (N. Murali, Y. Lin, Y. Mechulam, P. Plateau, and B. D. Nageswara Rao, submitted), and to the pyrophosphoryl transfer enzyme phosphoribosylpyrophosphate (PRPP) synthetase (Jarori *et al*., 1995). The glycosidic torsion angles ($O_{4'}-C_{1'}-N_9-C_8$) deduced for these complexes are all in the narrow range of $51 \pm 7°$, suggestive of a common motif for the recognition and binding of the adenosine moiety at the active sites of ATP-utilizing enzymes irrespective of the point of cleavage on the phosphate chain.

Complete characterization of the structure of the enzyme-bound nucleotide requires information regarding the orientation of the phosphate chain with respect to the adenosine moiety, which has not been obtained, thus far, for any of the ATP-utilizing enzymes. Such information can be obtained through relaxation measurements of ^{13}C and ^{15}N nuclei in the adenosine moiety, which will enable the determination of their distances from the paramagnetic cation coordinated with the phosphate chain. However, the experiments require nucleotides specifically labeled with ^{13}C and ^{15}N to high isotopic enrichment, which was a deterrent factor in attempting these measurements. As an initial step, we synthesized [2-^{13}C]-labeled ATP and ADP at 99% enrichment (Nageswara Rao & Ray, 1992).

This paper presents structural measurements on Mn(II)-[2-^{13}C]ATP and Mn(II)[2-^{13}C]ADP bound to rabbit muscle creatine kinase. The contribution of the lifetimes of the E·M·S complexes to the ^{13}C relaxation rates observed for enzyme-bound complexes was assessed on the basis of frequency and temperature dependence of the relaxation rates. The Mn(II)−[2-^{13}C] distances calculated from the relaxation data were interpreted, together with our previously published Co(II)−^{31}P distances and TRNOESY-determined adenosine conformations for these complexes, with the help of molecular modeling. Conformational searches coupled with CHARMm energy calculations were used to determine a family of nucleotide conformations compatible with all of the available structural data. Of particular interest in this context is the ability to monitor possible differences in the conformations of MnATP and MnADP on the enzyme which may be indicative of the changes occurring at the active site as a result of the phosphoryl transfer.

EXPERIMENTAL PROCEDURES

Materials. ADP, ATP, 0.1 mM $MnCl_2$ solution in 0.15 M NaCl, ATP-Sepharose, rabbit muscle lactate dehydrogenase, and pyruvate kinase were obtained from Sigma Chemical Co., Hepes was from Research Organics, Raney nickel was from Aldrich, [^{13}C]formaldehyde (99% ^{13}C) was from Cambridge Isotope Laboratories, and Chelex-100 was from Bio-Rad Laboratories. All other chemicals used were of analytical reagent grade.

Labeled Compound Syntheses. [2-^{13}C]AMP was formed from AMP by a series of steps with intermediate chromatographic purification over Dowex-1 (formate). AMP was initially oxidized to the 1-oxide with monopermaleic acid (Mantsch *et al*., 1975). This was followed by ring opening to the carboxamidoxime, reduction over Raney nickel to give the carboxamidine, and ring closure with [^{13}C]formaldehyde to give the labeled AMP (Meyer & Wong, 1981).

[2-^{13}C]ATP was synthesized by enzymatic phosphorylation of [2-^{13}C]AMP as described previously (Nageswara Rao & Ray, 1992) with the one change of using ATP-Sepharose instead of free, unlabeled ATP to initiate the reaction. Thus, the [2-^{13}C]ATP produced had 99% isotopic enrichment with yields of 90%−95%.

[2-^{13}C]ADP was enzymatically synthesized from [2-^{13}C]-ATP by hexokinase transfer of the terminal phosphate to glucose followed by a DEAE-Sephadex chromatography, similar to that used in ATP purification (Nageswara Rao & Ray, 1992). Typical yields of [2-^{13}C]ADP were 90%−95% with 99% isotopic abundance.

Enzyme Preparation. Creatine kinase was purified from the rabbit skeletal muscles by method B of Kuby et al. (1954). The enzyme so purified was subjected to an additional gel filtration chromatography on a Sephadex-G75 column to remove adenylate kinase (Jarori et al., 1985). The specific activity of the enzyme at this stage was between 50 and 70 units/mg. The enzyme was finally dialyzed against 50 mM Hepes-K^+, pH 8.0, containing pre-equilibrated Chelex-100 resin to eliminate trace metal ions from the sample. The enzyme was concentrated up to ∼240−300 mg/mL in an Amicon ultrafiltration cell (model 8010). Protein and nucleotide concentrations were determined spectrophotometrically, with $\epsilon_{280}^{mg/mL} = 0.896$ cm^{-1} and a dimer molecular weight of 81 000 (Noda et al., 1954) for the enzyme, and $\epsilon_{259}^{mM} = 15.4$ cm^{-1} for ATP and ADP. A Beckman Altex model 3500 digital pH meter was used for pH measurements. No correction was applied for the isotopic effect of D_2O on the pH. All the buffer and ligand solutions were passed through a Chelex-100 column to eliminate trace paramagnetic impurities.

NMR Measurements. ^{13}C NMR measurements on [2-^{13}C]-ATP complexes at 75 MHz were made on an NTC-300 wide-bore NMR spectrometer equipped with a 12-mm multinuclear probe, a 293 C pulse programmer, a Nicolet 1280 computer, and a variable temperature controller. A typical sample contained ∼0.8 mL of the enzyme in an 8-mm o.d. NMR sample tube placed inside a 12-mm NMR tube. D_2O for field-frequency lock was added between the two tubes. Measurements on [2-^{13}C]ATP complexes at 50 and 125 MHz were made on NTC-200 and VXRS-500 spectrometers at the Purdue University Biochemical Magnetic Resonance laboratory.

^{13}C NMR measurements on [2-^{13}C]ADP complexes at 75 and 125 MHz were made on UNITY-300 and UNITY-500 spectrometers with high-stability variable temperature controllers, 10-mm multinuclear probes from Cryomagnet Systems, and SUN Microsystems SPARC station 5/85 host computers. ^{13}C NMR measurements on [2-^{13}C]ADP complexes at 50 MHz were made on a 200 MHz spectrometer based on a Bruker magnet refitted by Cryomagnet Systems,

[2] In the case of adenylate kinase, however, the data indicate β,γ-bidentate binding of the cation in the enzyme−metal−ATP complex, and β-monodentate binding in the enzyme−metal−GDP complex. The distance of α-P to the cation is ∼1.0 Å longer than that for direct coordination in both cases (Ray *et al*., 1988).

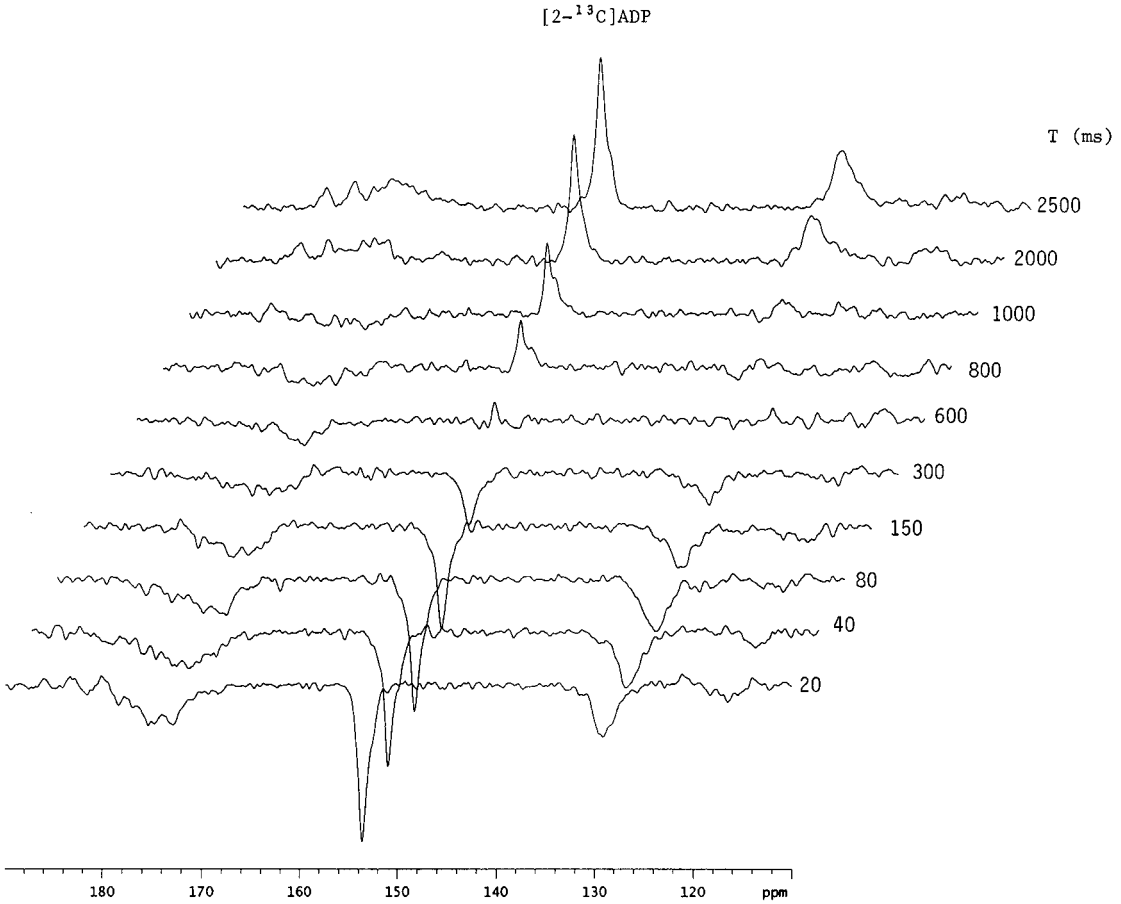

FIGURE 1: Typical T_1 measurement at 125 MHz for [2-^{13}C]ADP bound to creatine kinase in the presence of Mn(II) ($p = 8.64 \times 10^{-3}$). NMR parameters: $\pi/2$ pulse width, 22 μs; sweep width, 25 790 Hz; data size, 8192; line broadening, 60 Hz; number of scans, 448; and recycle delay, 2.66 s. The delay times (T) used in the T_1 measurement are given in the figure. Unidentified resonances are due to natural abundance ^{13}C of carbonyls and aromatics in the enzyme. Computer fit gave a T_1 value of 0.74 s and a standard deviation of ~0.04 s.

a 10-mm multinuclear probe from Cryomagnet Systems, and a console constructed by retuning the NTC-300 console, described above, to 200 MHz. For these measurements, a typical sample contained ~1.6 mL of the enzyme in a 10-mm o.d. NMR sample tube with a 5-mm o.d. NMR sample tube held concentrically inside to contain D_2O for field-frequency lock.

T_1 measurements were made using a standard inversion recovery sequence with a composite π pulse (Levitt, 1982). Frequency-modulated broad-band decoupling was used to obtain proton-decoupled ^{13}C spectra.[3] A typical spectral stack plot used for T_1 measurement is shown in Figure 1. The ^{13}C relaxation time in the diamagnetic complex E·[2-^{13}C]ADP is 0.82 s. The T_1 values are about 0.3−0.4 s for the highest Mn(II) concentrations used. The recycle delay of 2.66 s chosen in these measurements is larger by a factor of 3.25 than the largest T_1 value, rather than the customary factor of 5. This choice minimizes interference from sample-degrading effects, such as adventitious hydrolysis of nucleotides, by reducing the overall experimental time by one-third. At the same time, no noticeable impairment of the accuracy of the T_1 values for low Mn(II) concentrations resulted. Furthermore, the T_1 data, such as that in Figure 1, was analyzed by means of a three-parameter fit (Levy & Peat, 1975) which adequately corrects for any deviations from complete recovery at the end of recycle delay. The errors quoted for relaxation rates and activation energies are based on standard deviations given by computer fits and deviations between measurements made with independent samples.

Theoretical Details. The theory of nuclear spin relaxation in the presence of paramagnetic cations is well-known (Dwek, 1973; James, 1973; Mildvan & Gupta 1978; Burton *et al.*, 1979; Jardetzky & Roberts, 1981). A summary of this theory and the experimental strategy arising from it have previously been published (Jarori *et al.*, 1985, 1989; Ray & Nageswara Rao, 1988b; Ray *et al.*, 1988). The relevant equations for the analysis of the data in this paper are given below. Given a sample which contains two exchanging complexes, one paramagnetic and the other diamagnetic, with fractional concentrations p and $(1 - p)$ and nuclear relaxation rates $(T_{1M})^{-1}$ and $(T_{1D})^{-1}$, respectively, such that $(T_{1M})^{-1} \gg (T_{1D})^{-1}$, the observed relaxation rate is given by

$$(T_{1,\mathrm{obs}})^{-1} = \frac{(1-p)}{T_{1D}} \frac{T_{1M} + \tau_M}{T_{1M} + (1-p)\tau_M} + \frac{p}{T_{1M} + (1-p)\tau_M} \quad (1)$$

where τ_M is the lifetime of the paramagnetic complex. If $p \ll 1$, then eq 1 reduces to the commonly used form,

$$(T_{1P})^{-1} = p/(T_{1M} + \tau_M) \quad (2)$$

[3] The proton decoupling also avoids complications due to the differentially-broadened line shapes of the proton-coupled [2-^{13}C] doublet in the enzyme complexes (Nageswara Rao & Ray, 1992; see footnote 5).

Table 1: Paramagnetic Effect $(pT_{1p})^{-1}$ (s^{-1}) of Mn(II) on ^{13}C Relaxation Rates and the Corresponding Activation Energies (ΔE) (kcal/mol) for Mn[2-^{13}C]ATP and Mn[2^{13}C]ADP Complexes Bound to Rabbit Muscle Creatine Kinase and for Mn[2-^{13}C]ATP Free in Solution[a]

complex (sample composition)	NMR frequency (MHz)	relaxation rate $(pT_{1p})^{-1}$ (s^{-1})	activation energy ΔE (kcal/mol)
Mn[2-^{13}C]ATP			
([2-^{13}C]ATP, 2.99 mM; $MnCl_2$, 0.158−0.552 mM)	75	73.0 ± 2.0	2.0 ± 0.1
E·Mn[2-^{13}C]ATP			
(enzyme, 6.24 mM; [2-^{13}C]ATP, 5.01 mM; $MnCl_2$, 0.109−0.319 mM)	50	59.4 ± 3.0	
(enzyme, 5.85 mM; [2-^{13}C]ATP, 4.67 mM; $MnCl_2$, 0.077−0.375 mM)	75	55.6 ± 3.0	1.3 ± 0.2
(enzyme, 5.74 mM; [2-^{13}C]ATP, 5.17 mM; $MnCl_2$, 0.084−0.469 mM)	125	30.2 ± 2.0	
E·Mn[2-^{13}C]ADP			
(enzyme, 5.98 mM; [2-^{13}C]ADP, 4.8 mM; $MnCl_2$, 0.0288−0.253 mM)	50	104 ± 7.0	
(same sample as for 50 MHz)	75	48.1 ± 2.0	2.0±0.2
(enzyme, 5.2 mM; [2-^{13}C]ADP, 4.0 mM; $MnCl_2$, 0.0347−0.341 mM)	125	17.5 ± 0.5	

[a] Samples were in 50 mM Hepes-K^+, pH 8.0, and measurements were made at 21 ± 1 °C. The ΔE values were obtained from Arrhenius plots (see Figure 2). Measurements were made at four to five different values of $p = [E{\cdot}M{\cdot}S]/\{[E{\cdot}S] + [E{\cdot}M{\cdot}S]\}$.

Neglecting the contribution of scalar hyperfine interaction, T_{1M} is related to the cation−nucleus distance by

$$(T_{1M})^{-1} = (C/r)^6 f(\tau_C) \tag{3}$$

where

$$C = [(2/15)S(S+1)g^2\gamma_I^2\beta^2]^{1/6} \tag{4}$$

and

$$f(\tau_C) = 3\tau_{C1}/(1 + \omega_I^2\tau_{C1}^2) \tag{5}$$

for Mn(II) complexes (with $\omega_S\tau_{C2} \gg 1$). Also,

$$\tau_{Ci}^{-1} = \tau_R^{-1} + \tau_{Si}^{-1} \qquad i = 1, 2 \tag{6}$$

In eqs 4−6, S, g, and ω_S are, respectively, the spin, the g-factor, and the Larmor frequency for the cation, γ_I and ω_I are, respectively, the gyromagnetic ratio and the resonance frequency of the relaxing nucleus, β is the Bohr magneton, τ_R is the isotropic rotational correlation time of the complex, and τ_{S1} and τ_{S2} are the electronic longitudinal and transverse relaxation times of the paramagnetic cation. These equations assume an isotropic g-factor and that the zero-field splitting is smaller than the Zeeman interaction of the cation. These assumptions are valid for Mn(II) complexes. τ_{S1} is given by

$$\tau_{S1}^{-1} = B[\tau_v/(1 + \omega_S^2\tau_v^2) + 4\tau_v/(1 + 4\omega_S^2\tau_v^2)] \tag{7}$$

where B is a constant related to the square of the fluctuations in the crystal field interaction strength and τ_v is the correlation time for its modulation. It is implied that $\tau_v \ll \tau_{S1}$.

Experimental Strategy. By performing the experiments exclusively on enzyme-bound substrate complexes, it will be possible to limit the exchange to two complexes, E·S and E·M·S, as implied in eq 1, and maximize the contribution of E·M·S to $(T_{1P})^{-1}$. In order to ensure this requirement, sample conditions should be chosen such that [E] > [S] ≫ K_d, where K_d is the dissociation constant for the substrate. The concentrations chosen for the measurements presented here may be seen in Table 1. On the basis of the known dissociation constants for creatine kinase complexes (Reed et al., 1970), the fractional concentration of the paramagnetic complex free in solution ([M·S]/[E·M·S]) never exceeds ∼3%.

Since structural information is not available from measurements in which $\tau_M \gg T_{1M}$, and can be computed from measurements in which $\tau_M \approx T_{1M}$ only if τ_M is known, the contribution of τ_M to T_{1P} must be determined (see eqs 1 and 2). This was done by making T_{1P} measurements as a function of temperature in the range 7−35 °C and at three ^{13}C frequencies (50, 75, and 125 MHz). Note that the activation energies of T_{1M} are usually 1−3 kcal/mol while those for τ_M are 5−20 kcal/mol. Furthermore, T_{1M} depends on frequency and τ_M does not.

Molecular Modeling. Molecular modeling and energy calculations were performed using the CHARMm program (Brooks *et al*., 1983) in the software package QUANTA (4.1) running on a Silicon Graphics computer. The calculations were performed on an MnATP or MnADP complex in vacuum.

RESULTS AND ANALYSIS

Relaxation Data. For both the E·Mn[2-^{13}C]ATP and the E·Mn[2-^{13}C]ADP complexes, the values of $(pT_{1p})^{-1}$ obtained at 50, 75, and 125 MHz along with the activation energies (ΔE) determined at 75 MHz are presented in Table 1. Measurements made on the free MnATP complex at 75 MHz to determine the Mn(II)−2C distance in this complex are also included in Table 1.

The temperature dependencies of $(pT_{1p})^{-1}$ at 75 MHz were measured in the range of 7−35 °C (see Figure 2).[4] The activation energies obtained are $\Delta E = 1.3 \pm 0.2$ kcal/mol and $\Delta E = 2.0 \pm 0.2$ kcal/mol, respectively. Note that both of the Arrhenius plots in Figure 2 have positive slopes. If $(pT_{1p})^{-1}$ is exchange limited ($\tau_M \gg T_{1M}$), then an Arrhenius plot of $(pT_{1p})^{-1}$ vs $10^3/T$ will have a negative slope with an activation energy of 5−20 kcal/mol. On the other hand, if $T_{1M} \gg \tau_M$, then the temperature dependence of $(pT_{1p})^{-1}$ arises from $f(\tau_C)$, which acquires temperature dependence, in turn, through τ_R and τ_v, the latter of which governs τ_{S1} (see eqs 2−7). τ_R and τ_v decrease with increasing temperature with

[4] In both of the Arrhenius plots in Figure 2, the data points in the range of 15−20 °C noticeably deviate from the expected linearity. This type of deviation in the temperature dependence around 15−20 °C is consistent with previous NMR and EPR measurements on nucleotide complexes of both creatine kinase (McLaughlin *et al*., 1976; Nageswara Rao & Cohn, 1981) and arginine kinase (Jarori *et al*., 1989).

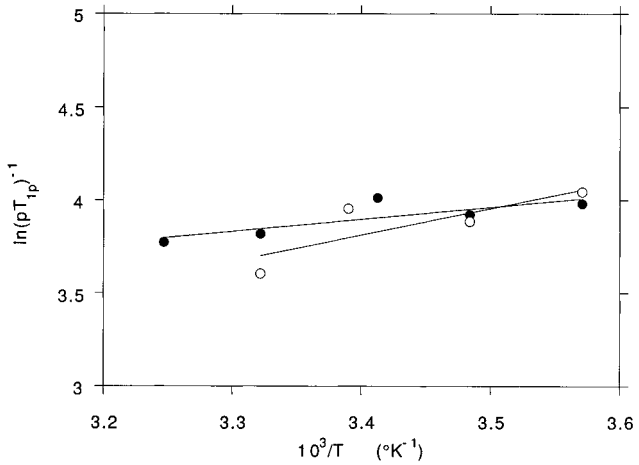

FIGURE 2: Temperature dependence of paramagnetic relaxation rate $(pT_{1p})^{-1}$ (s^{-1}) at 75 MHz for [2-^{13}C]ATP in E·Mn[2-^{13}C]ATP (●) and for [2-^{13}C]ADP in E·Mn[2-^{13}C]ADP (○). Typical sample conditions are given in Table 1. The activation energies are 1.3 ± 0.2 kcal/mol for E·Mn[2-^{13}C]ATP, and 2.0 ± 0.2 kcal/mol for E·Mn[2-^{13}C]ADP.

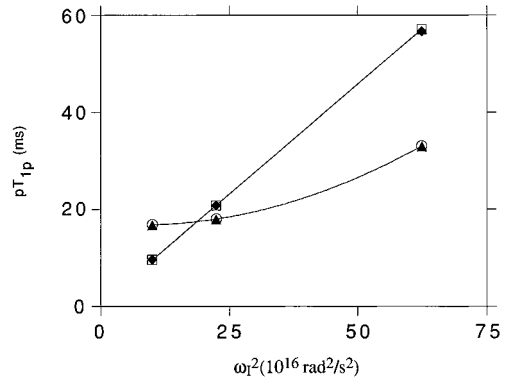

FIGURE 3: Frequency dependences of ^{13}C relaxation times (pT_{1p}) at 21 °C for E·Mn[2-^{13}C]ATP (○, ▲) and E·Mn[2-^{13}C]ADP (□, ◆). Experimental data points (○, □) shown are for 50, 75, and 125 MHz. Typical sample conditions are given in Table 1. Theoretical curves are drawn through the solid points (▲, ◆) calculated by using the parameters r = 10.0 Å, $B = 6.1 \times 10^{20}$ s^{-2}, and $\tau_v = 3.2 \times 10^{-13}$ s for E·MnATP and r = 8.6 Å, $B = 3.8 \times 10^{20}$ s^{-2}, and $\tau_v = 3.2 \times 10^{-14}$ s for E·MnADP, with C = 512 Å $s^{-1/3}$ for both.

a low activation energy of 1−3 kcal/mol. However, τ_{S1} may either decrease or increase with temperature depending on whether $\omega_S\tau_v \gg 1$ or $\omega_S\tau_v \ll 1$. Similary, $f(\tau_C)$ may be directly or inversely proportional to τ_{C1} depending on whether $\omega_I\tau_{C1} \ll 1$ or $\omega_I\tau_{C1} \gg 1$. Thus, in a general case, the slope of the Arrhenius plot of $(pT_{1p})^{-1}$ can be positive or negative, with activation energies in the range of 1−3 kcal/mol, characteristic of τ_R and τ_v. Observation of a positive slope in the Arrhenius plot with low activation energy is thus indicative of fast exchange. This is consistent with our earlier estimate of $\tau_M \approx 0.5$ ms (Jarori *et al*., 1985), which is much shorter than the shortest T_{1M} (16−17 ms at 50 MHz) reported here. Furthermore, both $(pT_{1p})^{-1}$ values exhibit strong frequency dependence in the range of 50−125 MHz (see Table 1 and Figure 3). Thus, it can be concluded that the pT_{1p} values have negligible contribution from τ_M and are essentially equal to T_{1M} (see eq 2). Therefore, the Mn(II)−2C distances are calculable from this data.

The plots of pT_{1p} vs ω_I^2, shown in Figure 3, for both the E·MnATP and E·MnADP complexes indicate that the magnitude of the relaxation times and their frequency dependencies are significantly different from each other. The plot is linear for the ADP complex and shows a curvature at lower frequencies for the ATP complex. It may be seen from eqs 2, 3, and 5 that if τ_{C1} is independent of frequency, pT_{1p} vs ω_I^2 will be linear with a slope of $(r/C)^6\tau_{C1}/3$ and an intercept of $[\tau_M + (r/C)^6/3\tau_{C1}]$. Frequency dependence of τ_{C1} arises through τ_{S1} (see eq 6), which in turn depends on frequency if $\omega_S\tau_v \geq 1$. Thus, the contrasting frequency dependencies in Figure 3 suggest that τ_{S1} is different in the two complexes and that $\omega_S\tau_v \geq 1$ for the ATP complex and $\omega_S\tau_v \ll 1$ for the ADP complex. A numerical fit of the data for both the complexes, on the basis of eqs 5 and 7 along with the use of eqs 2−4, yields the Mn(II)−2C distances in the two complexes listed in Table 2 along with the associated parameters B and τ_v (see eq 7). The distance between Mn(II) and the 2C of adenine is 10.0 ± 0.5 Å in E·MnATP and 8.6 ± 0.5 Å in E·MnADP.

Table 2: Mn(II)−2C Distances (r) and Parameters B and τ_v Obtained from the Numerical Fit of pT_{1p} vs ω_I^2 Data for MnATP and MnADP Complexes of Creatine Kinase[a] and the Value of r for Free MnATP

complex	distance (r, Å)	B (s^{-2})	τ_v (ns)
Mn[2-^{13}C]ATP[b]	6.5 ± 0.5		
E·Mn[2-^{13}C]ATP	10.0 ± 0.5	6.1×10^{20}	3.2×10^{-4}
E·Mn[2-^{13}C]ADP	8.6 ± 0.5	3.8×10^{20}	3.2×10^{-5}

[a] The numerical fit was performed using eqs 3−7 with C = 512 Å $s^{-1/3}$ for ^{13}C and Mn(II) and τ_R = 42 ns for creatine kinase (Nageswara Rao & Ray, 1992). [b] Distance calculated assuming a correlation time τ_{C1} of 0.1 ns in eq 5 (see footnote 6).

Note that the B and τ_v values obtained are significantly different for the two complexes. On the basis of these parameters the value of τ_{S1} in the two complexes at the three frequencies is in the range 1−12 ns. τ_R is estimated to be 42 ns (Nageswara Rao & Ray, 1992). Clearly τ_{S1} is the dominant correlation time for the electron−nucleus dipolar interaction. The various parameters involved can be used to rationalize the positive slopes observed in the Arrhenius plots presented in Figure 2. Also listed in Table 2 is the Mn(II)−2C distance calculated from the 75 MHz relaxation data for MnATP free in solution by assuming a correlation time τ_{C1} of 0.1 ns. Note that since the expected internal mobilities associated with the phosphate chain and the glycosidic rotation of free MnATP affect the Mn(II)−2C vector, the distance calculated is, perforce, mobility averaged (also see footnote 6).

Molecular Modeling. In order to deduce the conformations of the cation−nucleotide complex compatible with the distance data obtained above, a molecular modeling procedure is used in which previously obtained structural data from ^{31}P NMR and TRNOESY measurements on these complexes are incorporated. Thus, with the glycosidic torsion and sugar pucker set up in the manner determined by TRNOESY, and with the cation directly coordinated with all the phosphate groups, the orientation of the phosphate chain with respect to the adenosine moiety is determined by three rotations, $\gamma(O_{5'}-C_{5'}-C_{4'}-C_{3'})$, $\phi_1(C_{4'}-C_{5'}-O_{5'}-P_\alpha)$, and $\phi_2(C_{5'}-O_{5'}-P_\alpha-O_{\alpha\beta})$.

The first of these rotations, γ, may be deduced, in principle, from the TRNOESY data involving $H_{5'}$ and $H_{5''}$. However, the resonances of these two protons are superposed in the spectra. The NOE data, therefore, do not differentiate the two distances, r_{i1} and r_{i2}, of $H_{5'}$ and $H_{5''}$, respectively,

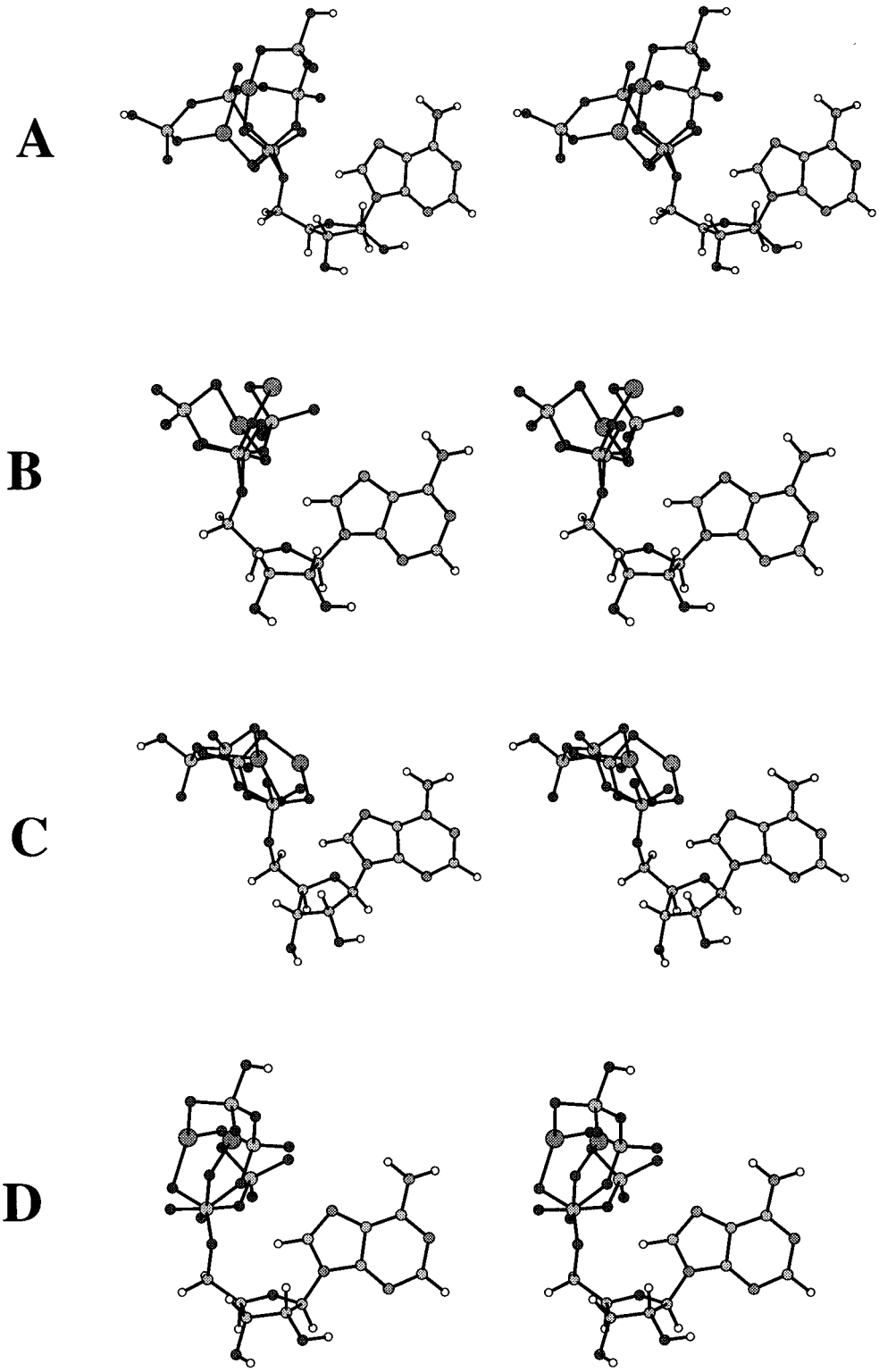

FIGURE 4: Stereoviews that illustrate the conformations compatible with the Mn(II)−2C distances of 10.0 ± 0.5 and 8.6 ± 0.5 Å in E·MnATP and E·MnADP complexes, respectively, for different combinations of the angles ϕ_1($C_{4'}-C_{5'}-O_{5'}-P_\alpha$), and ϕ_2($C_{5'}-O_{5'}-P_\alpha-O_{\alpha\beta}$). (A) Superposition of two ATP conformations with (ϕ_1,ϕ_2) = (120,120) and (130,−130). (B) Superposition of two ADP conformations with (120,60) and (130,−70). (C) Superposition of ATP (120,120) with ADP (120,60). (D) Superposition of ATP (130,−130) with ADP (130,−70).

from a third proton, *i*. γ is, therefore, arbitrary. However, an average distance, r_i, given by

$$r_i = \left[\frac{r_{i1}^{-6} + r_{i2}^{-6}}{2}\right]^{-1/6} \quad (8)$$

corresponding to half the initial slope of the observed NOE was calculated to fit the TRNOESY data for the superposed resonance (Murali *et al*., 1993). Note that r_i does not equal either r_{i1} or r_{i2}. In order to reduce the arbitrariness in γ, a conformational search was set up in which γ was varied in the range −180° to +180° in steps of 1° and the CHARMm energy was computed for each orientation. For each of these structures, the quantity

$$Q = \sum_i \left[\frac{r_{i1}^{-6} + r_{i2}^{-6}}{2r_i^{-6}} - 1 \right]^2 \quad (9)$$

is calculated. A range of values of γ which provides the best agreement with the observed NOE's of the superposed $H_{5'}$ and $H_{5''}$ resonances, i.e., the smallest values for Q, was identified. The lowest CHARMm energies of these low-Q structures occur in the range of $66 < \gamma < 78$. The energy variation in this range is minimal, and therefore the value of $\gamma = 72$, in the middle of the range, was chosen. Note that the TRNOESY data show that the conformation of the adenosine is the same in both E·MgATP and E·MgADP. This conformation has been refined further for the present computation by using QUANTA (4.1), which is an improved version of the program previously used by Murali *et al*. (1993). The various torsion and dihedral angles of the structure are given in Table 3.

A conformational search was then set up independently varying the two torsions, ϕ_1 and ϕ_2, in steps of 10° over the range −180° to +180°. For each of these 1369 structures, the CHARMm energy was computed and the distance between Mn(II) and the adenine 2C was measured. This modeling computation yielded virtually identical results for MnATP and MnADP complexes. From this rather large array of data, acceptable ranges for the two torsion angles were identified first by comparing the Mn(II)−2C distances in the model with the experimentally determined values and then by choosing among the ranges those with the least energy. Finally, the structures were discriminated on the criterion of minimal change required in the torsion angles, ϕ_1 and ϕ_2, to go from a structure representative of the Mn(II)−2C distance in the ATP complex to that in the ADP complex. This procedure yielded ϕ_1 in the range 120°−130° for both complexes. ϕ_2 has two acceptable ranges, 100°−120° and −130° to −150° for the ATP complex and 40°−60° and −70° to −90° for the ADP complex. Some of these conformations are shown in the superposed stereoviews juxtaposed in Figure 4. Figure 4A shows the two ATP conformations with $(\phi_1,\phi_2) = (120,120)$ and $(130,-130)$, and 4B the two ADP conformations with (120,60) and (130,−70). Figure 4C shows a superposition of the ATP conformation (120,120) with the ADP conformation (120,60), and Figure 4D has a similar superposition of ATP (130,−130) with ADP (130,−70). Together, these superposed structures depict the disparate conformations that are compatible with the distance data obtained thus far on the individual cation−nucleotide complexes of creatine kinase. Figures 4C and D show the differences between bound ATP and ADP. Between the superposed structures of ATP and ADP, the cation is displaced by ∼1.7Å.

Table 3: Various Torsion Angles in the Adenosine Moiety Obtained by Refinement of TRNOE Data of Creatine Kinase Complexes of ATP and ADP[a]

designation	torsion	angle (deg)
χ	$O_{4'}-C_{1'}-N_9-C_8$	46
ν_0	$C_{4'}-O_{4'}-C_{1'}-C_{2'}$	−9
ν_1	$O_{4'}-C_{1'}-C_{2'}-C_{3'}$	14
ν_2	$C_{1'}-C_{2'}-C_{3'}-C_{4'}$	−13
ν_3	$C_{2'}-C_{3'}-C_{4'}-O_{4'}$	8
ν_4	$C_{3'}-C_{4'}-O_{4'}-C_{1'}$	1
γ	$O_{5'}-C_{5'}-C_{4'}-C_{3'}$	72

$P = \tan^{-1}\{[(\nu_4 + \nu_1) - (\nu_3 + \nu_0)]/[2\nu_2(\sin 36° + \sin 72°)]\} = 158.2°$

[a] The TRNOE data is from Murali *et al*. (1993). The definitions used for various torsion angles are the same as described by Sanger (1984). P is the pseudorotation phase angle. Since ν_2 is negative, 180° was added to the P value computed (Altona & Sundaralingam, 1972).

DISCUSSION

A considerable amount of data is now available regarding the location of the cation with respect to the phosphate chain and on the conformation of the adenosine in the nucleotides bound to phosphoryl transfer enzymes. The orientation of the phosphate chain with respect to adenosine forms the missing information required for complete characterization of the structure of enzyme-bound nucleotides. Paramagnetic relaxation measurements with Mn(II) offer a reliable means for gathering this data for cation−nucleus distances larger than ∼6.5 Å. For shorter distances, the relaxation rates with Mn(II) are exchange-limited (Jarori *et al.*, 1985). In addition, Mn(II) is preferable to Co(II) from the point of view of the applicability of the theory to evaluate the cation−nucleus distances from the relaxation data. Frequency-dependent relaxation measurements analyzed on the basis of eqs 2−7 yield accurate values of the distances provided that the assumption of a single conformation described by a single correlation time is appropriate. In this context, the question of internal mobility of the nucleotide needs to be examined. The Mn(II)−2C distance is readily affected by the glycosidic torsion, as well as the mobility of the phosphate chain. Both of these motions are known to occur in MgATP and MgADP, free in solution, with large amplitude and low activation energy. Evidence that these mobilities are arrested in the enzyme complexes was obtained from the differentially broadened line shape of the proton-coupled [2-^{13}C] doublet of the ATP complexes of six different enzymes of molecular mass ranging from 20 kDa (adenylate kinase) to 240 kDa (pyruvate kinase) (Nageswara Rao & Ray, 1992).[5] It is therefore, plausible to describe the reorientation of the Mn(II)−[2-^{13}C] dipolar vector through $f(\tau_C)$ (see eq 5) with a single τ_C. Nevertheless, the presence of some degree of conformational heterogeneity and low-amplitude internal mobility cannot be entirely ruled out. As long as such factors cause a minor change in the cation−nucleus distance (r) of interest,[6] the effect on the accuracy is not serious in view of the r^{-6} dependence of T_{1M} (see eq 3).

From the point of view of the structure of the enzyme-bound cation−nucleotide complexes, the two Mn(II)−2C

[5] Differential broadening of the proton-coupled ^{13}C doublet of [2-^{13}C] nucleotides arises due to interference effects between the two ^{13}C relaxation mechanisms, viz., ^{13}C−^{1}H dipolar interaction and ^{13}C chemical shift anisotropy (CSA) as they are both second-rank tensor interactions. The line width difference depends on the principal values and relative orientations of these two tensors in addition to τ_R. Experimental measurements of the ^{13}C CSA tensor of [2-^{13}C]AMP provided information on all the parameters except τ_R, so that τ_R can be calculated from the ^{13}C line shapes of bound [2-^{13}C]ATP in the enzyme complexes (Nageswara Rao & Ray, 1992).

[6] If the conformational heterogeneity and internal mobility lead to significant excursions in the value of r, then the relaxation data will yield a distance closer to the shorter r values. Conversely, if the distances calculated correspond to an extended conformation, it is unlikely that these factors contribute significantly to the measured relaxation rates. By the same token, the relatively short Mn(II)−2C distance of 6.5 Å computed for free MnATP suggests that the mobilities of the phosphate chain and the glycosidic rotation occurring in this complex modulate this vector and affect the relaxation data.

distances of 10.0 ± 0.5 Å in the ATP complex and 8.6 ± 0.5 Å in the ADP complex are clearly the important parameters obtained. Qualitatively, these distances show that the phosphate chains of ATP and ADP assume extended conformations on the enzyme. More specifically, the conformational searches for compatible structures assisted by CHARMm energy calculations significantly narrowed the acceptable ranges for the two angles $\phi_1(C_{4'}-C_{5'}-O_{5'}-P_\alpha)$, and $\phi_2(C_{5'}-O_{5'}-P_\alpha-O_{\alpha\beta})$ on the basis of just the two Mn(II)−2C distances obtained for bound ATP and ADP. The difference between the Mn(II)−2C distances in ATP and ADP complexes was used in the choice of acceptable structures with the criterion that the conformational alterations accompanying phosphoryl transfer occur with an economy in motion, i.e., through minimal and least complicated changes in the angles ϕ_1 and ϕ_2. This criterion is reasonable but not precise. A determination of the precise conformation of the phosphate chain of bound nucleotides with respect to the adenosine moiety requires distance data for several nuclei on the adenyl and ribosyl moieties with respect to the cation. Such data will provide both confirmatory as well as dicriminatory constraints for the choice of compatible conformations. Measurements are currently in progress to obtain this data by using nucleotides labeled at other positions, the synthesis of which has recently been completed.

The significant difference of 1.4 Å in the Mn(II)−2C distances in enzyme-bound E·MnATP and E·MnADP and the displacement of the cation by 1.7 Å between the two structures are indicative of the conformational adjustments accompanying the interconversion of reactants and products on the enzyme surface. We recently investigated whether structural alterations of this kind could be studied by making relaxation measurements in enzyme-bound equilibrium mixtures in the presence of the paramagnetic cation. The interpretation of such relaxation data will be complicated by the interconversion rates but is amenable to analysis under some experimentally-realizable conditions (Nageswara Rao, 1995; B. D. Ray, S. B. Landy, and B. D. Nageswara Rao, unpublished experiments). Information on the structural changes, such as the movement of the itinerant phosphoryl group, accompanying the enzyme turnover should be of value in understanding the enzyme mechanism.

ACKNOWLEDGMENT

We thank Ms. Marie-Ann Bertrand, Chemistry Department, IUPUI, for the synthesis of [2-^{13}C]AMP and Dr. Daniel H. Robertson of the Computational Facility for Molecular and Biomolecular Science, IUPUI, for helpful suggestions.

REFERENCES

Altona, C., & Sundaralingam, M. (1972) *J. Am. Chem. Soc. 94*, 8205−8212.
Brooks, B. R., Bruccoleri, R. E., Olafson, B. D., States, D. J., Swaminathan, S., & Karplus, M. (1983) *J. Comp. Chem. 4*, 187−217.
Burton, D. R., Forsen, S., Karlstrom, G., & Dwek, R. A. (1979) *Prog. Nucl. Magn. Reson. Spectrosc. 13*, 1−45.
Dwek, R. A. (1973) *NMR in Biochemistry*, Chapters 9 and 10, Clarendon, Oxford, U.K.
James, T. L. (1973) *NMR in Biochemistry*, pp 177−210, Academic, New York.
Jardetzky, O., & Roberts, G. C. K. (1981) *NMR in Molecular Biology*, Chapter 3, Academic, New York.
Jarori, G. K., Ray, B. D., & Nageswara Rao, B. D. (1985) *Biochemistry 24*, 3487−3494.
Jarori, G. K., Ray, B. D., & Nageswara Rao, B. D. (1989) *Biochemistry 28*, 9343−9350.
Jarori, G. K., Murali, N., & Nageswara Rao, B. D. (1994) *Biochemistry 33*, 6784−6791.
Jarori, G. K., Murali, N., & Nageswara Rao, B. D. (1995) *Eur. J. Biochem. 230*, 517−524.
Kuby, S. A., Noda, L., & Lardy, H. A. (1954) *J. Biol. Chem. 209*, 191−201.
Levitt, M. H. (1982) *J. Magn. Reson. 48*, 234−264.
Levy, G., & Peat, I. (1975) *J. Magn. Reson. 18*, 500−521.
Leyh, T. S., Goodhart, P. J., Nguyen, A. C., Kenyon, G. L., & Reed, G. H. (1985) *Biochemistry 24*, 308−316.
Mantsch, H. H., Goia, I., Kezdi, M., Barzu, O., Dansoreanu, M., Jebeleanu, G., & Ty, N. G. (1975) *Biochemistry 14*, 5593−5601.
McLaughlin, A. C., Leigh, J. S., Jr., & Cohn, M. (1976) *J. Biol. Chem. 251*, 2777−2787.
Meyer, R. B., Jr., & Wong, C. G. (1981) *J. Labelled Compds. Radiopharm. 18*, 1119−1122.
Mildvan, A. S., & Gupta, R. K. (1978) *Methods Enzymol. 49*, 322−359.
Moore, J. M., & Reed, G. H. (1985) *Biochemistry 24*, 5328−5333.
Murali, N., Jarori, G. K., & Nageswara Rao, B. D. (1993) *Biochemistry 32*, 12941−12948.
Murali, N., Jarori, G. K., & Nageswara Rao, B. D. (1994) *Biochemistry 33*, 14227−14236.
Nageswara Rao, B. D. (1995) *J. Mag. Reson., Ser. B 108*, 289−293.
Nageswara Rao, B. D., & Cohn, M. (1981) *J. Biol. Chem. 256*, 1716−1721.
Nageswara Rao, B. D., & Ray, B. D. (1992) *J. Am. Chem. Soc. 114*, 1566−1573.
Noda, L., Kuby, S. A., & Lardy, H. A. (1954) *J. Biol. Chem. 209*, 203−210.
Ray, B. D., & Nageswara Rao, B. D. (1988a) *Biochemistry 27*, 5574−5578.
Ray, B. D., & Nageswara Rao, B. D. (1988b) *Biochemistry 27*, 5579−5585.
Ray, B. D., Rösch, P., & Nageswara Rao, B. D. (1988) *Biochemistry 27*, 8669−8676.
Reed, G. H., Cohn, M., & O'Sullivan, W. J. (1970) *J. Biol. Chem. 245*, 6547−6552.
Reed, G. H., & Cohn, M. (1972) *J. Biol. Chem. 247*, 3073−3081.
Reed, G. H., & Leyh, T. S. (1980) *Biochemistry 19*, 5472−5480.
Sanger, W. (1984) in *Principles of Nucleic Acid Structure* (Cantor, C. R., Ed.) pp 9−28, Springer-Verlag, New York.
Villafranca, J. J. (1984) *Phosphorous-31 NMR: Principles and Applications* (Gorenstein, D. G., Ed.) pp 155−174, Academic Press, New York.

BI9602573